Structural Heterogeneity and Coordination Chemistry of Nickel(II) Octaethyl-*meso*-nitroporphyrins

J. D. Hobbs,*,† S. A. Majumder,†,‡ L. Luo,§ G. A. Sickelsmith,§ J. M. E. Quirke,*,§ C. J. Medforth,∥ K. M. Smith,∥ and J. A. Shelnutt*,†,‡

Contribution from the Fuel Science Department, Sandia National Laboratories, Albuquerque, New Mexico 87185-0710, Department of Chemistry, University of New Mexico, Albuquerque, New Mexico 87131, Department of Chemistry, Florida International University, Miami, Florida 33199, and Department of Chemistry, University of California, Davis, California 95616

Received October 27, 1993®

Abstract: The role of steric crowding of peripheral substituents in causing nonplanar distortions of the porphyrin macrocycle has been investigated in a series of nickel(II) *meso*-nitrooctaethylporphyrins as models for protein-induced nonplanar distortions of metal–tetrapyrrole cofactors. UV–visible absorption spectra, resonance Raman spectra, nuclear magnetic resonance spectra, and molecular mechanics calculations are given for nickel(II) derivatives of 5-mono-, 5,15-di-, 5,10-di-, 5,10,15-tri-, and 5,10,15,20-*meso*-nitro-substituted octaethylporphyrins. The frequencies of the structure-sensitive Raman lines are found to shift to lower energies in response to sterically induced nonplanar distortion of the porphyrin macrocycle rather than in response to the addition of a strong electron-withdrawing nitro substituent. The Raman spectra of all except tetranitrooctaethylporphyrin show spectroscopic evidence of heterogeneity resulting from the presence of conformers with differing degrees of nonplanarity. Evidence from UV–visible absorption spectra, nuclear magnetic resonance spectra, and molecular mechanics calculations suggests that nickel tetranitrooctaethylporphyrin in solution may exhibit conformers with different types of nonplanar distortions which however do not differ in the relative degree of distortion. We find that the effect of increasing distortion on the chemical reactivity with axial ligating agents, which normally acts to lower the affinity, is overcome in the case of the nitrooctaethylporphyrin series by the increasing electron depletion of the porphyrin ring as the number of nitro substituents increases.

Introduction

The structural and electronic effects of peripheral substitution of the porphyrin macrocycle have been the subject of numerous theoretical and experimental inquiries.[1-4] In particular, the nonplanar macrocyclic distortions which result from steric interactions among the peripheral substituents have been investigated in order to understand similar nonplanar distortions observed in various biological systems that contain porphyrins and related tetrapyrroles. These nonplanar conformations have been postulated to play a functional role in reactions carried out in the photosynthetic reaction centers,[5] the photosynthetic antenna system of *Prosthecochloris aestuarii*,[6] methylreductase[7], vitamin B_{12} and B_{12} dependent enzymes,[8] and heme proteins.[9]

An interesting example of the relevance of nonplanar distortions of the porphyrin prosthetic group has been reported for *c*-type cytochromes.[10] An analysis of high-resolution X-ray crystal structures for cytochromes *c* isolated from seven species reveals the presence of a strongly conserved nonplanar distortion of the hemes that is induced through covalent linkages between the heme peripheral substituents and two cysteine amino acid residues of the protein. This mechanism of induced distortion is further supported by molecular mechanics calculations which show that the nonplanar distortion is maintained only in the protein environment. More generally, a recent resonance Raman study of metal-substituted octaethyl- and 5-nitrooctaethylporphyrins indicates that nonplanar distortions in porphyrins that contain large metals like iron occur only at the expense of significant energy.[11] Thus, for the case of cytochromes *c*, the presence of a conserved nonplanar distortion, maintained at the expense of significant protein energy, suggests a functional role for the nonplanar heme. Heme planarity changes can result from changes in metal redox state occurring during electron transfer or from alterations in the proteins tertiary structure that accompany the protein–protein binding of mitochondrial *c*-type cytochromes to their physiological redox partners.

The nonplanar distortions of tetrapyrroles that occur naturally in proteins can be induced in model porphyrins by crowding of the peripheral substituents as, for example, in the case of the dodeca-substituted porphyrins. Changes in the chemical, electronic, and vibrational properties that occur in response to nonplanar conformational distortions associated with steric crowding at the porphyrin periphery have been correlated with a wide variety of structural parameters obtainable from molecular mechanic calculations and X-ray crystallographic data.[12] The nonplanar distortions include the ruffled and saddle conformations of the porphyrin macrocycle defined by Scheidt and Lee.[13] These distortions influence porphyrin ring geometry as well as interactions of the central metal with the pyrrole nitrogens and axial

† Sandia National Laboratories.
‡ University of New Mexico.
§ Florida International University.
∥ University of California, Davis.
® Abstract published in *Advance ACS Abstracts*, March 15, 1994.

(1) Gouterman, M. *J. Chem. Phys.* **1959**, *30*, 1139.
(2) Shelnutt, J. A. *J. Chem. Phys.* **1980**, *72*, 3948.
(3) Shelnutt, J. A.; Ortiz, V. *J. Phys. Chem.* **1985**, *89*, 4733.
(4) Davis, D. G. In *The Porphyrins*; Dolphin, D., Ed.; Academic Press: New York, 1978; Vol. 5, p 127.
(5) Barkigia, K. M.; Chantranupong, L.; Smith, K. M.; Fajer, J. *J. Am. Chem. Soc.* **1988**, *110*, 7566–7567.
(6) Tronrud, D. E.; Schmid, M. F.; Matthews, B. W. *J. Mol. Biol.* **1986**, *188*, 443–454.
(7) (a) Furenlid, L. R.; Renner, M. W.; Smith, K. M.; Fajer, J. *J. Am. Chem. Soc.* **1990**, *112*, 1634–1635. (b) Furenlid, L. R.; Renner, M. W.; Smith, K. M.; Fajer, J. *J. Am. Chem. Soc.* **1990**, *112*, 8987–8989.
(8) Geno, M. K.; Halpern, J. *J. Am. Chem. Soc.* **1987**, *109*, 1238–1240.
(9) Alden, R. G.; Ondrias, M. R.; Shelnutt, J. A. *J. Am. Chem. Soc.* **1990**, *112*, 691–697.
(10) Hobbs, J. D.; Shelnutt, J. A. *Arch. Biochem. Biophys.* **1993**, submitted for publication.
(11) Anderson, K. K.; Hobbs, J. D.; Luo, L.; Stanley, K. D.; Quirke, J. M. E.; Shelnutt, J. A. *J. Am. Chem. Soc.* **1993**, *115*, 12346–12352.
(12) Shelnutt, J. A.; Medforth, C. J.; Berber, M. D.; Barkigia, K. M.; Smith, K. M. *J. Am. Chem. Soc.* **1991**, *113*, 4077.
(13) Scheidt, W. R.; Lee, Y. J. *Struct. Bonding* **1987**, *64*, 1.

0002-7863/94/1516-3261$04.50/0 © 1994 American Chemical Society

ligands. Furthermore, these structural changes influence chemical processes such as the binding and release of axial ligands and the oxidation and reduction of the porphyrin and central metal ion.[5,14,15] These processes are, in turn, important to the catalysis of many physiologically important chemical and photochemical reactions.

Molecular mechanics (MM) calculations of the structures of some dodeca-substituted porphyrins successfully predicted the nonplanar distortions observed in the X-ray crystal structures.[12,16] These nonplanar distortions were also correlated with changes in the resonance Raman and UV–visible spectra of these compounds. Further MM studies of these highly substituted porphyrins have examined the effects of the central metal in relation to core size and specific out-of-plane distortions of the macrocycle.[16] From these initial studies, an intricate picture of the role played by peripheral steric interactions on modes of porphyrin distortion begins to emerge. These steric interactions and their effect on macrocycle conformation are influenced by the type, size, the shape of the substituents. Further, the orientation of the substituent with respect to the macrocycle and other substituents gives rise to multiple conformers (local minima) which depending on there relative energies may or may not be observed. The steric interactions, for some porphyrins, result in a single more or less rigid conformation while, for other porphyrins, result in the coexistance of multiple conformations at room temperature. Our goal is to improve the understanding of the factors governing the appearance of multiple conformers and develop the spectroscopic methods required to investigate the presence of these conformers in proteins and determine their role in biological function.

In this work we have examined the structural and electronic effects of the progressive addition of NO_2 groups at the *meso*-carbon positions of nickel(II) derivatives of octaethylporphyrin (NiOEP) using molecular mechanics calculations, UV–visible absorption spectroscopy, nuclear magnetic resonance spectroscopy, and resonance Raman spectroscopy. Results are presented for the nickel derivatives of 5-, 5,15-, 5,10-, 5,10,15-, and 5,10,15,20-nitro-substituted octaethylporphyrins, shown in Figure 1, and some cobalt(II) derivatives. We also investigated the effect of out-of-plane distortions on specific chemical properties, in this case the axial ligand affinity of the central Ni(II) ion.

Materials and Methods

Preparation of Mono-, Di-, and Trinitrooctaethylporphyrins. 5-Nitrooctaethylporphyrin, 5,10-dinitrooctaethylporphyrin, and 5,15-dinitrooctaethylporphyrin were prepared by the method of Bonnett and Stephenson.[17] 5,10,15,20-tetranitrooctaethylporphyrin was prepared by the method of Gong and Dolphin.[18] Nickel(II) and cobalt(II) complexes of nitrooctaethylporphyrins were prepared using the standard literature procedures of Buchler.[19]

Molecular Mechanics Calculations. Energy optimized porphyrin structures were determined using POLYGRAF (Version 3.1) software (Molecular Simulation, Inc.) with a force field that is based upon potential energy functions described previously and force constants obtained from a recent normal coordinate analysis of NiOEP.[20] The development of the force field has been described in detail elsewhere.[12] In this work, the following changes were implemented: (1) electrostatic terms were included in calculating the total energy, (2) the van der Waals potential energy term for the hydrogen atoms was changed from a Lenard–Jones 6–12 to an exponential (r^{-6}) functional form, and (3) a cutoff distance of 50 Å (rather than 9 Å) was employed in calculations of electrostatic and van der Waals potential energy terms. These changes did not significantly affect the calculated structures, but they did alter significantly the ordering of the optimized energies for the various comformers possible as a result of different initial ethyl group orientations. Partial atomic charges used in determining the contribution of the electrostatic energy to the total energy were calculated using the charge equilibration method of Rappé and Goddard.[21] Electrostatic charges were updated periodically during the energy minimzations using this method.

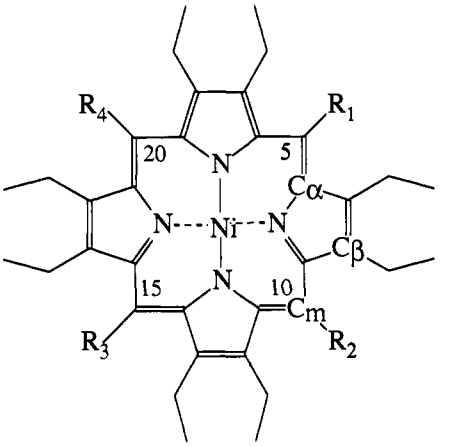

Nickel Porphyrin	R_1	R_2	R_3	R_4
OEP	H	H	H	H
OEMNP	NO_2	H	H	H
OE5,15DNP	NO_2	H	NO_2	H
OE5,10DNP	NO_2	NO_2	H	H
OEtriNP	NO_2	NO_2	NO_2	H
OETNP	NO_2	NO_2	NO_2	NO_2

Figure 1. Chemical structures of nickel(II) *meso*-nitroporphyrins.

Resonance Raman Spectroscopy. Dual-channel resonance Raman spectra were obtained using the 413.1-nm line from a Krypton ion laser (Coherent, Inc.) as the excitation source. The scattered light was collected at 90° to the direction of propagation and polarization of the exciting laser beam. During the scattering experiment, the partitioned Raman cell was rotated at 50 Hz to prevent sample heating. Sample concentrations were typically in a range of 1×10^{-5} to 1×1^{-4} M. Laser powers were 60 mW at the quartz cell. Resonance Raman spectra of pairs of the nickel porphyrins were obtained simultaneously using a dual-channel Raman spectrometer described elsewhere.[22] The spectrometer slits were adjusted to obtain a 3–4-cm^{-1} band pass.

The nitroporphyrin derivatives were dissolved in CS_2 or CH_2Cl_2, and 200-mL aliquots were added to each side of a dual-compartment quartz cell. No porphyrin decomposition was observed in the two noncoordinating solvents (CH_2Cl_2 and CS_2) during the approximately 20–30-min duration of a scan. NiOETNP was found to decompose during the Raman experiment in all coordinating solvents except methanol. The other nickel nitroporphyrins were photostable in all coordinating solvents used. Sample integrity was monitored by examination of selected single scans of the Raman spectrum obtained during signal averaging and by UV–visible

(14) (a) Kratky, C.; Waditschatka, R.; Angst, C.; Johansen, J.; Plaquerent, J. C.; Schreiber, J.; Eschenmoser, A. *Helv. Chim. Acta* **1982**, *68*, 1312–1320. (b) Waditschatka, R.; Kratky, C.; Juan, B.; Heinzer, J.; Eschenmoser, A. *J. Chem. Soc., Chem. Commun.* **1985**, 1604–1605.

(15) (a) Kadksh, K. M.; Caemelbecke, E. V.; D'Souza, F. D.; Medforth, C. J.; Smith, K. M.; Tabard, A.; Guilard, R. *Organometallics* **1993**, *12*, 2411–2413. (b) Kadish, K. M.; Caemelbecke, E. V.; Boulas, P.; D'Souza, F. D.; Vogel, E.; Kisters, M.; Medforth, C. J.; Smith, K. M. *Inorg. Chem.* **1993**, *32*, 4177–4178.

(16) Sparks, L. D.; Medforth, C. J.; Park, M.-S.; Chamberlain, J. R.; Ondrias, M. R.; Senge, M. O.; Smith, K. M.; Shelnutt, J. A. *J. Am. Chem. Soc.* **1993**, *115*, 581–592.

(17) Bonnett, R.; Stephenson, G. F. *J. Org. Chem.* **1965**, *30*, 2791.

(18) (a) Gong, L.-C.; Dolphin, D. *Can. J. Chem.* **1985**, *63*, 401. (b) Gong, L.-C.; Dolphin, D. *Can. J. Chem.* **1985**, *63*, 406.

(19) (a) Buchler, J. W. Static Coordination of Metalloporphyrins. In *Porphyrins and Metalloporphyrins*; Smith, K. M., Ed.; Elsevier: Amsterdam, 1975; pp 157–231. (b) Buchler, J. W. Synthesis and Properties of Metalloporphyrins. In *The Porphyrins*; Dolphin, D., Ed.; Academic Press: New York, 1978; Vol. 1, pp 389–483.

(20) (a) Li, X.-Y.; Czernuszewicz, R. S.; Kincaid, J. R.; Stein, P.; Spiro, T. G. *J. Phys. Chem.* **1990**, *94*, 47. (b) Li, X.-Y.; Czernuszewicz, R. S.; Kincaid, J. R.; Stein, P.; Spiro, T. G. *J. Am. Chem. Soc.* **1989**, *111*, 7012.

(21) Rappé, A. K.; Goddard, W. A., III. *J. Phys. Chem.* **1991**, *95*, 3358.

(22) Shelnutt, J. A. *J. Phys. Chem.* **1983**, *87*, 605.

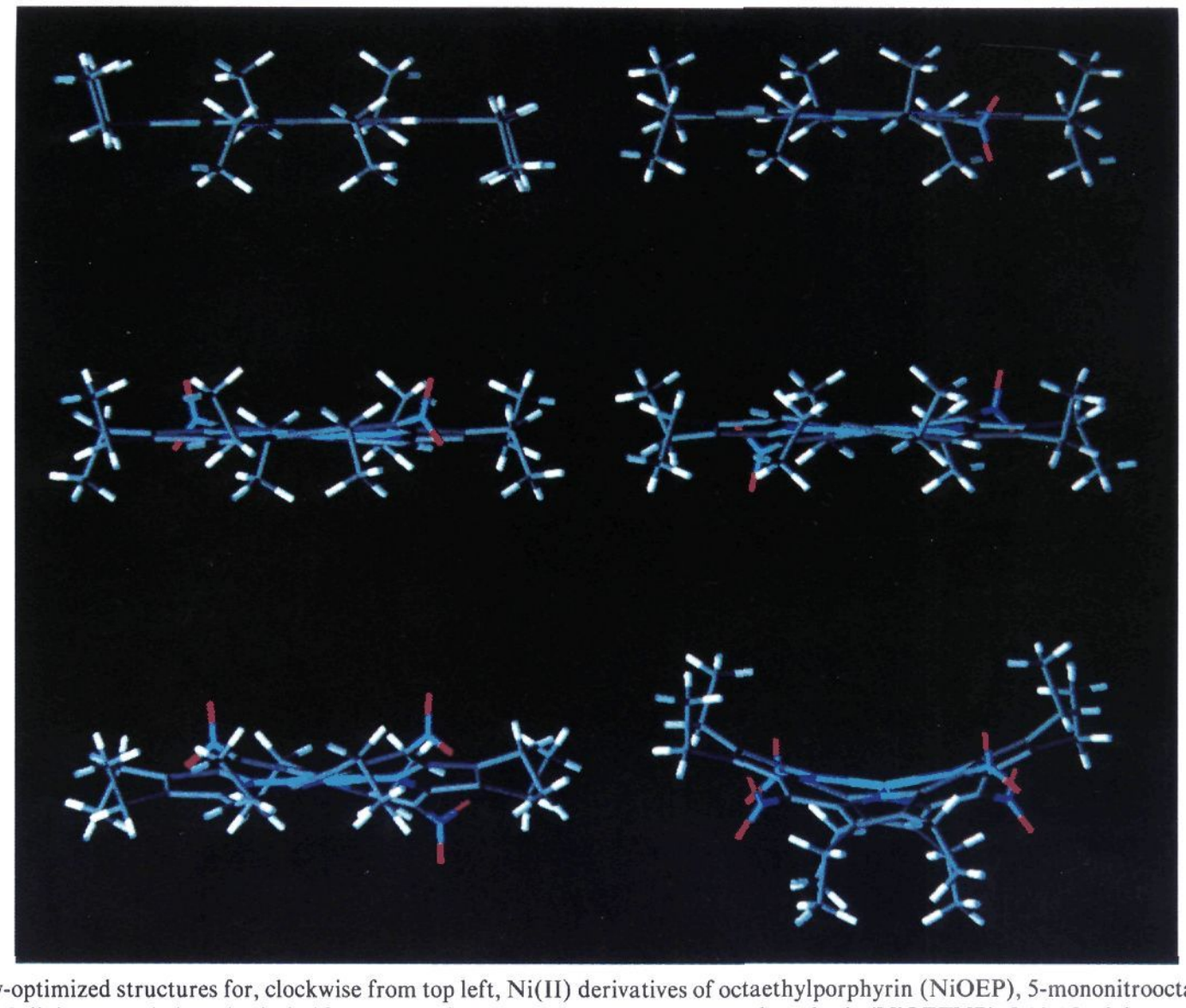

Figure 2. Energy-optimized structures for, clockwise from top left, Ni(II) derivatives of octaethylporphyrin (NiOEP), 5-mononitrooctaethylporphyrin (NiOEMNP), 5,15-dinitrooctaethylporphyrin (NiOE5,15DNP), 5,10,15,20-tetranitrooctaethylporphyrin (NiOETNP), 5,10,15-trinitrooctaethylporphyrin (NiOEtriNP), and 5,10-dinitrooctaethylporphyrin (NiOE5,10DNP).

absorption spectra taken before and after exposure to laser light. UV–visible absorption spectra were obtained using an HP8452 (Hewlett-Packard) diode array spectrophotometer.

Poprhyrin vibrational frequencies were taken from the peak positions of the lines in fast-Fourier-transform smoothed spectra. The Raman lines were decomposed into component Lorentzian lines using a nonlinear, least-squares curve-fitting program in which the frequencies, peak intensities, line widths, the linear background were allowed to vary. The ν_{10} Raman line for this series showed anomalously broad, asymmetric line shapes, and, therefore, two Lorentzian components were used in fitting this line; although, for the mono- and dinitro OEP derivatives, three line shapes gave statistically better fits. A single Lorentzian line was assumed for all other lines even though some broadening was observed in other Raman lines besides ν_{10}.

NMR Spectroscopy. Proton NMR spectra of H_2OETNP, H_4OETNP^{2+}, NiOETNP, and CoETNP were measured at a frequency of 300 MHz. CD_2Cl_2 was used as the solvent for H_2OETNP and NiOETNP. H_4OETNP^{2+} was made by adding trifluoroacetic acid (1% by volume) to H_2OETNP in CD_2Cl_2. In all cases the solvent peak (5.30 ppm) was used as an internal standard. The variable temperature unit was calibrated using a sample of methanol.[23]

Results

Molecular Mechanics Calculations. Calculated structures of these porphyrins are shown in Figures 2 and 3, and relevant calculated structural parameters for this series are shown in Table 1. In general, the calculated Ni–N distances decrease with an increase in nonplanarity of the porphyrin macrocycle (Table 1). This trend is similar to that seen for the nickel octaalkyltetraphenylporphyrins.[12,16] Core size (a projection of the Ni–N bond into the average plane of the macrocycle) also decreases with an increase in the nonplanar distortion of the macrocycle. In our results nonplanarity is measured by several other parameters. The N–Ni–N bond angle across the porphyrin (opposite pyrrole nitrogens) is related to the amount of pyrrole tilting in the saddle distortion of the metalloporphyrin. In the saddle form, the *meso*-carbons (C_m) remain in the mean porphyrin plane and the pyrrole rings are alternately displaced above and below the mean plane. The C_α–N–N–C_α dihedral angles, defined as the twist angle in Table 1, reflect a ruffling of the macrocycle induced by opposite pyrroles twisting about the M–N bonds. These two angles give an estimate of the two general types of distortion observed in metalloporphyrins.[13] For this series of Ni(II) porphyrins, increases in both pyrrole tile and pyrrole twist are generally noted in the calculated structures. The root-mean-square out-of-plane (RMS OOP) distance reported in Table 1 gives a single, comprehensive measure of the degree of nonplanar distortion of the macrocycle. RMS OOP distances consistently increase with each additional *meso*-nitro-substitution and appear to be a reliable measure of the overall degree of distortion of the macrocycle regardless of whether the distortion type is saddle, ruffled, or a mixture of the two.

For this porphyrin series, the initial orientation of the pyrrole ethyl substituents was found to affect both structure and total energy; that is, the energy optimized structure obtained depended on the initial ethyl orientations (local minima). Two adjacent ethyl groups on a single pyrrole or on neighboring pyrroles may be oriented in either cis or trans positions. For each *meso*-nitro-substituted isomer, ethyl orientations were adjusted initially to match those reported for the NiOEP and nickel(II) 2,3,7,8,12,-13,17,18-octaethyl-5,10,15,20-tetraphenylporphyrin (NiOETPP) crystal structures. Additional ethyl configurations were then investigated to determine which of the conformers had the lowest energy (global minimum). Each optimized structure shown in Figure 2 is found to be the lowest energy conformer of the calculated series. For mono-, di-, and trinitro-substituted OEPs, the overall conformation of the macrocycle varied little for these different ethyl-group conformers. However, for tetranitro OEP,

(23) van Gleet, A. L. *Anal. Chem.* **1970**, *42*, 679.

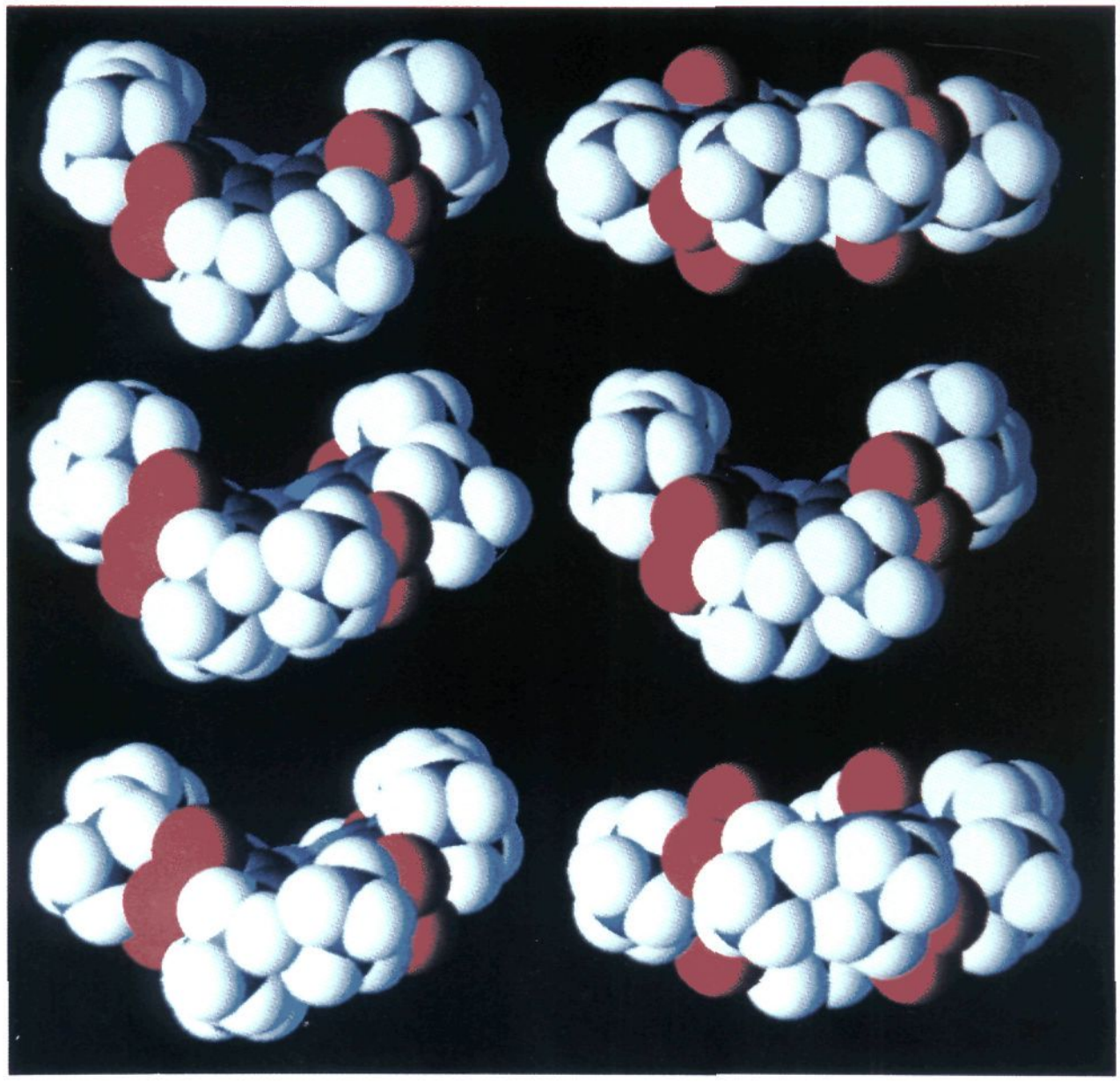

Figure 3. Energy-optimized structures within 2.0 kcal/mol of the lowest energy structure for nickel(II) 5,10,15,20-tetranitrooctaethylporphyrin (NiOETNP). The top four structures have differing ethyl orientations (cis *versus* trans). The bottom two structures have ethyl orientations identical to those found in the crystal structure.[39]

Table 1. Calculated Structural Parameters for the Nickel(II) *meso*-Nitroporphyrin Series

Ni(II) porphyrin	core size (Å)	Cα–N–Cα angle (deg)	N–Ni–N angle (deg)[a]	twist angle (deg)[b]	RMS OOP dev (Å)[c]
OEP	1.946	104.4	180.0	0.1	0.015
OEMNP	1.957	104.5	179.7	4.9	0.081
OE5,15DNP	1.964	104.8	179.7	13.4	0.164
OE5,10DNP	1.960	105.0	179.8	18.3	0.199
OEtriNP	1.937	106.1	179.8	37.0	0.384
OETNP	1.917	105.8	162.0	16.3	0.685

[a] The N–Ni–N angle across the porphyrin (180° for a planar porphyrin) shows the amount of doming in the metalloporphyrins. [b] The twist of the pyrrole rings as defined by the dihedral angles between opposite N–C_α bonds on opposite pyrroles. [c] Root-mean-squared out-of-plane deviation from the mean plane of the C_β, C_α, C_m, and N atoms of the porphyrin.

ethyl orientations had a more dramatic effect on macrocyclic distortions, particularly the relative twist of the pyrrole rings about the Ni–N bonds (ruffling). In fact, at least six distinct conformers (shown in Figure 3) with C_α–N–N–C_α angles varying from approximately 1.1 to 50.9° had total energies that spanned only 2.0 kcal/mol. Interestingly, macrocyclic distortion, as measured by the RMS OOP distances, remained remarkably consistent within these strutures (0.6 ± 0.1 Å).

UV–Visible Absorption Spectra. The absorption spectra for this series of nickel porphyrins in noncoordinating (CH_2Cl_2 and CS_2) and coordinating solvents (piperidine, pyridine, and methanol) are displayed in Figures 4 and 5, and the peak positions of the α (Q(0–0)), β (Q(0–1)), and γ (Soret or B(0–0)) bands are summarized in Table 2. In all solvents systems, the presence of each additional nitro group causes a bathochromic shift in the observed band positions. The Soret band, in particular, is also observed to broaden significantly with increasing *meso*-substitution. The red shift and band broadening with the increasing number of nitro substituents are observed for all absorption bands in both the four- and six-coordinate species.

The addition of nitro groups also has a clear effect upon the reactivity of the central nickel ion. Nickel octaethylporphyrin does not readily bind axial ligands. Even in the presence of strong nitrogenous bases, such as piperidine (pK_a = 2.80), NiOEP remains mostly four-coordinate.[24] Addition of only one *meso*-nitro group to NiOEP results in complete conversion of NiOEMNP to the six-coordinate complex in neat piperidine (Figure 4). This effect is magnified for the case of NiOETNP and results in the binding of relatively weak ligands such as methanol (see Table 2).

A strong UV band (in the range 347–370 nm) is observed for all *meso*-nitro-substituted OEPs upon formation of the hexacoordinated complex (Figure 4). This band was found to red shift and increase in intensity (relative to the Soret band) with increased nitro substitution. The presence of this band may be due either to the presence of a porphyrin-to-NO_2 charge-transfer band or to an increase in absorbance of a porphyrin π-to-π*

(24) (a) Shelnutt, J. A.; Alston, K.; Ho, J.-Y.; Yu, N.-T.; Yamamoto, T.; Rifkind, J. M. *Biochemistry* **1986**, *25*, 620. (b) Findsen, E. W.; Shelnutt, J. A.; Ondrias, M. R. *J. Phys. Chem.* **1988**, *92*, 307.

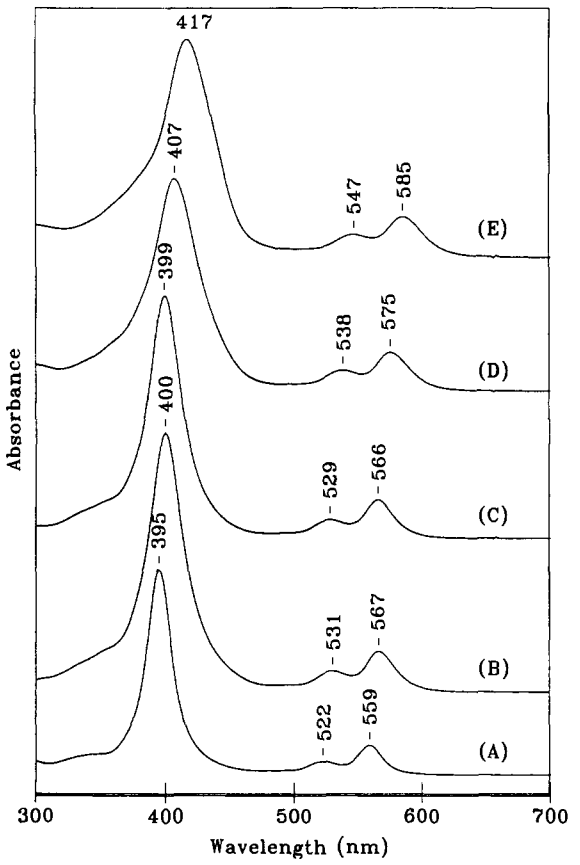

Figure 4. UV–visible absorption spectra of Ni(II) derivatives of (A) 5-nitrooctaethylporphyrin (NiOEMNP), (B) 5,10-dinitrooctaethylporphyrin (NiOE5,10DNP), (C) 5,15-dinitrooctaethylporphyrin (NiOE5,15DNP), (D) 5,10,15-trinitrooctaethylporphyrin (NiOEtRiNP), and (E) 5,10,15,20-tetranitrooctaethylporphyrin (NiOETNP) in dichloromethane.

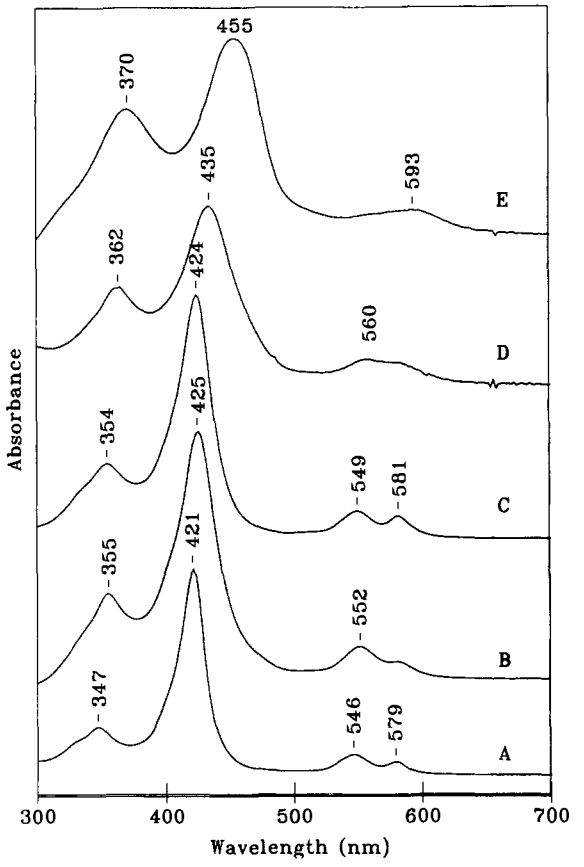

Figure 5. UV–visible absorption spectra of Ni(II) derivatives of (A) 5-nitrooctaethylporphyrin (NiOEMNP), (B) 5,10-dinitrooctaethylporphyrin (NiOE5,10DNP), (C) 5,15-dinitrooctaethylporphyrin (NiOE5,15DNP), (D) 5,10,15-trinitrooctaethylporphyrin (NiOEtRiNP), and (E) 5,10,15,20-tetranitrooctaethylporphyrin (NiOETNP) in piperidine.

transition that results from interactions between molecular orbitals of the porphyrin and those of the NO_2 group. INDO/s molecular orbital calculations for NiOETNP show porphyrin-to-nitro charge-transfer transitions to the blue of the Soret band.[25]

Resonance Raman Spectra. Representative high-frequency, resonance Raman spectra for the *meso*-nitro-substituted NiOEP series dissolved in CS_2 are shown in Figure 6, and frequencies of major Raman lines are summarized in Table 3. These lines are labeled upon the basis of a normal coordinate analysis of NiOEP.[26] Using Soret excitations, these modes correspond to in-plane skeletal vibrations of the macrocycle having A_{1g} and B_{2g} symmetries in the D_{4h} point-group representation.

The resonance Raman spectra of the nitro OEPs are similar to those observed for NiOEP.[11,27,28] Relative to NiOEP, the structure-sensitive vibrational modes ν_{10}, ν_2, ν_3, and ν_4 shift to lower frequencies with increased *meso*-substitution. As was previously observed for the nickel(II) octaalkyltetraphenylporphyrins,[12] the magnitude of the shift is proportional to the frequency of the mode. For example, the highest frequency mode, ν_{10}, shifts the most (42 cm^{-1}) going from the spectrum of the mononitro-substituted (1647 cm^{-1}) to that of the tetranitro-substituted complex (1605 cm^{-1}). The modes ν_2, ν_3, and ν_4 have total shifts of 20, 26, and 9 cm^{-1}, respectively, for this comparison.

Meso-nitro substitution also produces several new modes in the Raman spectra as compared with that of NiOEP. In particular, the presence of a new polarized mode at 1363 cm^{-1} in the spectrum of NiOEMNP (Figure 6A) may be associated with the symmetric stretch of the NO_2 moiety. (The NO_2 symmetric stretch is observed at 1355 cm^{-1} for nitrobenzene and is also polarized.)[11] This mode also shifts to lower frequency with increasing nitro substitution and is thus influenced by changes in the porphyrin structure. An additional depolarized mode at 1540 cm^{-1} in the spectrum of NiOEMNP (Figure 6A), but not present in the spectrum of NiOEP, may be the asymmetric NO_2 stretch. Although a similar mode is observed in the spectra for each of the *meso*-nitroporphyrins, its position does not shift in a predictable manner, making analogous assignment problematic. However, a similar pattern of frequency shifts in the infrared spectra were observed for zinc *meso*-nitro OEPs and attributed to the NO_2 group.[29] Isotopic substitution studies with $^{15}NO_2$ are in progress to clarify the assignments.

The resonance Raman spectra of the mono-, 5,15-di-, 5,10-di-, and trinitro complexes (Figure 6, parts A, B, C, and D, respectively) also offer evidence of structural heterogeneity among the porphyrin comformers in solution. Structural marker lines, ν_{10}, ν_2, and ν_3, are broader even than those observed for NiOEP which has been shown to exist in solution as a mixture of planar and nonplanar forms.[28] This effect is evident in an analysis of ν_{10}, which exhibits the most pronounced band broadening, using a curve-fitting procedure similar to those previously applied to the Raman spectra of NiOEP and NiOEMNP.[11] For these compounds, it was found that ν_{10} could be decomposed into two component lines corresponding to a high-frequency, planar conformer and a low-frequency, nonplanar conformer. The "natural" line widths of the planar and nonplanar forms were found to be approximately 11 and 16 cm^{-1}, respectively. Thus,

(25) Hobbs, J. D.; Shelnutt, J. A. Unpublished results.
(26) (a) Kitagawa, T.; Abe, M.; Ogoshi, H. *J. Chem. Phys.* **1978**, *69*, 4516. (b) Abe, M.; Kitagawa, T.; Kyogoku, Y. *J. Chem. Phys.* **1978**, *69*, 4526.
(27) Brennan, T. D.; Scheidt, W. R.; Shelnutt, J. A. *J. Am. Chem. Soc.* **1988**, *110*, 3919.
(28) Alden, R. G.; Crawford, B. A.; Doolen, R.; Ondrias, M. R.; Shelnutt, J. A. *J. Am. Chem. Soc.* **1989**, *111*, 2070–2072.
(29) Watanabe, E.; Nishimura, S.; Ogoshi, H.; Yoshida, Z. *Tetrahedron* **1976**, *31*, 1385–1390.

Table 2. Wavelength of Absorption maxima (nm) of the Nickel(II) *meso*-Nitroporphyrin Series in Various Coordinating and Noncoordinating Solvents

	dichloromethane			carbon disulfide			piperidine			pyridine			methanol		
Ni(II) porphyrin	γ	β	α	γ	β	α	γ	β	α	γ	β	α	γ	β	α
OEP															
4-coord	391	515	551	406	522	558	396		552						
6-coord							419	542	574						
OEMNP															
4-coord	395	522	559	406	527	563				402			392	520	556
6-coord							422	546	580	422	548	578			
OE5,15DNP															
4-coord	400	529	566	410	534	570									
6-coord							426	552	582	424	552	586			
OE5,10DNP															
4-coord	400	528	566	410	532	568							396	528	564
6-coord							424	550	582	424	550	582			
OEtriNP															
4-coord	406	538	575	418	540	578									
6-coord							434	558	585	432	560		416	552	574
OETNP															
4-coord	416	547	585	424	548	586									
6-coord							455		592	455		592	432		574

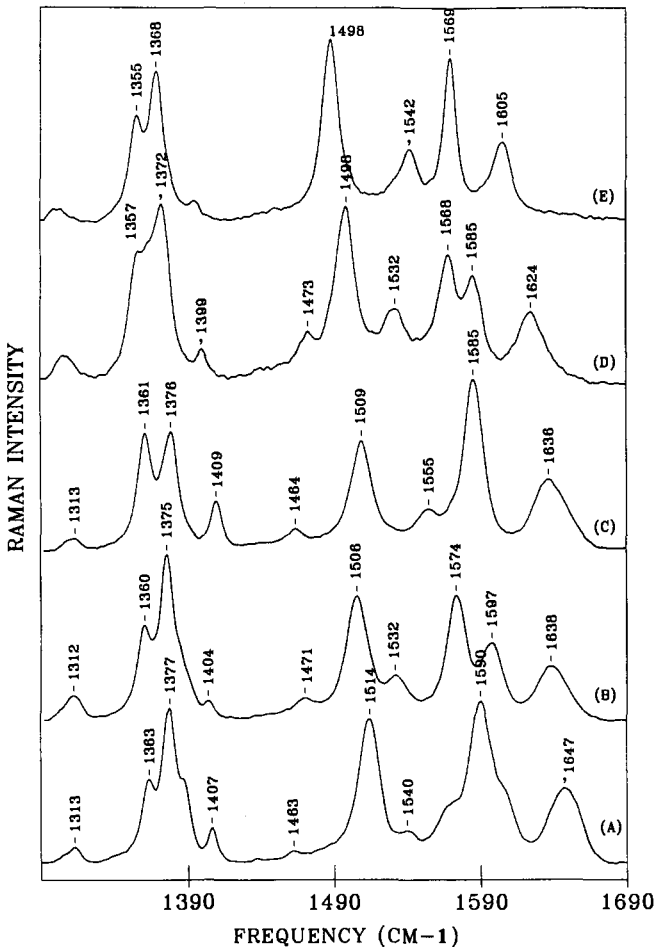

Figure 6. Resonance Raman spectra of Ni(II) derivatives of (A) 5-nitrooctaethylporphyrin (NiOEMNP), (B) 5,10-dinitrooctaethylporphyrin (NiOE5,10DNP), (C) 5,15-dinitrooctaethylporphyrin (NiOE5,15DNP), (D) 5,10,15-trinitrooctaethylporphyrin, and (E) 5,10,15,20-tetranitrooctaethylporphyrin (NiOETNP).

in order to accurately compare the structural heterogeneities for the nickel di-, tri-, and tetranitrooctaethylporphyrins, with those observed for NiOEP and NiOEMNP, and line widths of high-frequency planar components of ν_{10} were restricted to having line widths of between 11 and 16 cm^{-1}. The results of this analysis are summarized in Table 3. In general, it was observed that Raman line ν_{10} of all Ni nitro-substituted octaethylporphyrins, except NiOETNP, could be reasonably fit by two component lines having line separations (>7 cm^{-1}) and line widths comparable to those for NiOEP and NiOEMNP. A comparison of peak areas for these component lines suggests that, in contrast to observations for NiOEP, the populations of the more nonplanar, low-frequency conformers of NiOEMNP, NiOE5,15DNP, NiOE5,10DNP, and NiOEtriNP progressively dominate in solution. For NiOETNP, only a single nonplanar conformer can be justified using this fitting procedure.

NMR Spectra. Variable-temperature proton NMR spectroscopy has recently been used to study the solution conformations of many dodeca-substituted porphyrins.[30] The temperature dependence of the proton NMR spectra of H_2OETNP, H_4OETNP^{2+}, and NiOETNP was therefore investigated in the hope of obtaining information about the solution conformation of these porphyrins.

At 298 K, the spectrum of NiOETNP (data not shown) consisted of a quartet (CH_2; 3.20 ppm) and a triplet (CH_3; 1.15 ppm). At 178 K, the spectrum was essentially unchanged, with the signals showing only the slight broadening usually seen in low-temperature studies. The spectrum of H_4OETNP^{2+} also consisted of a quartet (CH_2; 3.15 ppm) and a triplet (CH_3; 0.95 ppm), and again there was only modest broadening at the lowest temperature studied (183 K). In contrast, the proton NMR spectrum of H_2OETNP as a function of temperature (Figure 7) did show changes that were characteristic of an exchange process. At 297 K, the CH_2 protons gave one quartet at 3.33 ppm, whereas at 184 K, two quartets of equal intensity were seen at 3.34 and 3.12 ppm. The coalescence temperature was 273 K, which, using the standard equation,[31] gave ΔG^*_{273} = 13.2 kcal mol^{-1}. At 297 K, the CH_3 protons were seen as a triplet at 1.23 ppm, but at 184 K, two triplets of equal intensity were noted at 1.12 and 1.01 ppm. The coalescence temperature of 263 K gave ΔG^*_{263} = 13.1 kcal mol^{-1}. The dynamic process seen for H_2OETNP was assigned as NH tautomerism because two ethyl signals of equal intensity were observed in the slow exchange spectrum and because the observed value of ΔG^* is similar to that measured for NH tautomerism in other free base dodeca-substituted porphyrins[30]

(30) (a) Medforth, C. J.; Berber, M. D.; Smith, K. M.; Shelnutt, J. A. *Tetrahedron Lett.* **1990**, *31*, 3719. (b) Barkigia, K. M.; Berber, M. D.; Fajer, J.; Medforth, C. J.; Renner, M. W.; Smith, K. M. *J. Am. Chem. Soc.* **1990**, *112*, 8851. (c) Medforth, C. J.; Smith, K. M. *Tetrahedron Lett.* **1990**, *31*, 5583. (d) Cheng, R.-J.; Chen, Y.-R.; Chuang, C.-E. *Heterocycles* **1992**, *34*, 1. (e) Medforth, C. J.; Senge, M. O.; Smith, K. M.; Sparks, L. D.; Shelnutt, J. A. *J. Am. Chem. Soc.* **1992**, *114*, 9859. (f) Senge, M. O.; Medforth, C. J.; Sparks, L. D.; Shelnutt, J. A.; Smith, K. M. *Inorg. Chem.* **1993**, *32*, 1716–1723.

(31) Abraham, R. J.; Fisher, J.; Loftus, P. *Introduction to NMR Spectroscopy*; Wiley: Chichester, U.K., 1988.

Table 3. Various Raman Modes (cm^{-1}) for Nickel(II) *meso*-Nitroporphyrins[a]

Ni(II) porphyrin	ν_4	ν_3	ν_2	ν_{10}	NP/P, ν_{10}	% NP	ν_{NO_2}	solvent
OEP	1383	1520	1603	1656	*1651/1658*	*49*		CS_2
OEMNP	1377	1513	1589	1647	*1644/1654*	*74*	1363	CS_2
	1354	1476					1369	pyr
	1356	1477	1572				1369	pip
OE510DNP	1378	1509	1585	1636	*1637/1646*	*76/24*	1361	CS_2
OE515DNP	1375	1506	1573	1638	*1635/1648*	*81/19*	1360	CS_2
OEtriNP	1372	1498		1624	*1624/1634*	*92/8*	1357	CS_2
	1351			1606			1371	MeOH
OETNP	1368	1488	1570	1605	*1604*	*100/0*	1355	CS_2
	1348						1367	pyr
	1349						1369	MeOH
OETPP	1360	1504	1562					CS_2

[a] NP = nonplanar form. P = planar form.

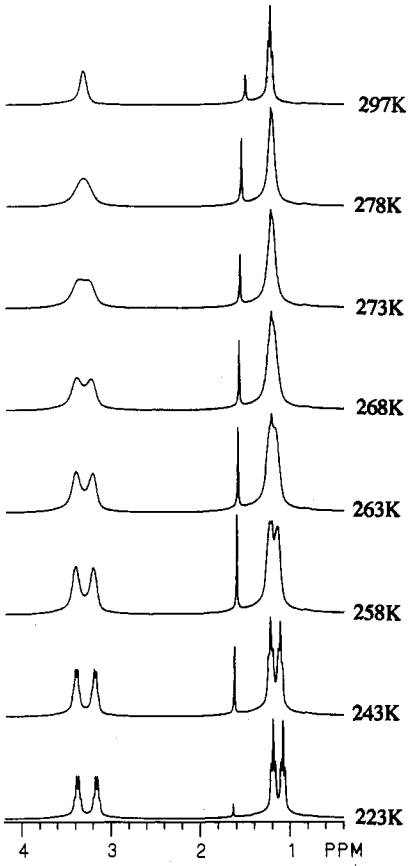

Figure 7. 300-MHz proton NMR spectra of H_2OETNP in CD_2Cl_2 obtained at the indicated temperatures.

and in 5,10,15,20-tetraphenylporphyrin (TPP).[32] It is significant that macrocyclic inversion was not detected for H_2OETNP, H_4-OETNP^{2+}, and NiOETNP, whereas it has been observed for many other dodeca-substituted porphyrins.[30] The structural implications of this result for the OETNP complexes are discussed in the next section.

Proton NMR spectroscopy was also used to study the solution conformation of the cobalt(II) complex of OETNP. In several cobalt(II) porphyrins, the paramagnetic shifts have been shown to be predominantly dipolar in nature.[33] Paramagnetic shifts have been used to obtain information about the solution structures of cobalt(II) porphyrins by comparing the shift ratios with geometric ratios calculated using the standard dipole equation.[34-36] Good agreement between the shift and geometric ratios implies that the structure used to calculate the geometric ratios is a reasonable approximation of the solution structure.

This procedure has previously been applied to cobalt(II) 2,3,7,8,12,13,17,18-octaethyl-5,10,15,20-tetraphenylporphyrin (CoOETPP).[37] The shift ratios for the ethyl protons in CoOETPP can be obtained by subtracting the chemical shifts of diamagnetic NiOETPP from those of CoOETPP and then normalizing the data by making the methylene shift equal to 10.0. In $CDCl_3$, the shift ratio for the methylene and methyl protons was found to be 10.0 to −0.8, compared to 10.0 to −0.4 in C_6D_6. Both of these shift ratios compare favorably with geometric ratios calculated from the crystal structure of CoOETPP[16] (10.0 to −1.5) or a molecular mechanics structure[16] (10.0 to −1.2). If one ethyl on each pyrrole is switched to an equatorial position, then the geometric ratios, based on a molecular mechanics structure, are 10.0 to +11.6 (equatorial) and 10.0 to −0.6 (axial). The axial orientations of the ethyl groups observed in crystal structures of CoOETPP therefore seem to be retained in solution.[16,30b,38]

We wondered whether a similar procedure would yield useful information about the solution conformation of CoOETNP. Using NiOETPP as a reference compound, the paramagnetic shift ratios for the methylene and methyl protons in CoOETNP were found to be 10.0 to +6.2 in CD_2Cl_2 and 10.0 to +7.6 in C_6D_6. Molecular mechanics calculations yielded geometric ratios of 10.0 to +0.7 (for an all axial saddle), 10.0 to +1.0 (for an axial ethyl from a mixed axial/equatorial saddle), and 10.0 to +10.8 (for an equatorial ethyl from a mixed axial/equatorial saddle) for NiOETNP. The observed shift ratios evidently agree better with the geometric ratio expected for a mixture of axial and equatorial ethyl groups, which is consistent with the crystal structure of NiOETNP.[39] However, an equally valid explanation for the shift ratios is a ruffled macrocyclic structure, which gives a geometric ratio of 10.0 to +6.6 for NiOETNP. In summary, if the paramagnetic shifts in CoOETNP are assumed to be predominantly dipolar in nature, they are indicative of increased conformational flexibility in comparison to CoOETPP. However, these shifts cannot be used to differentiate between multiple conformations of the macrocycle or the ethyl groups.

Discussion

Molecular Modeling Calculations. The ability to accurately model peripheral interactions and their influence upon porphyrin structures and dynamics is a necessary first step to developing detailed models of porphyrin/protein or porphyrin/substrate

(32) Abraham, R. J.; Hawkes, G. E.; Smith, K. M. *Tetrahedron Lett.* **1974**, *16*, 1483.
(33) LaMar, G. N.; Walker, F. A. *J. Am. Chem. Soc.* **1973**, *95*, 1790.
(34) Clayden, N. J.; Moore, G. R.; Williams, R. J. P.; Baldwin, J. E.; Crossley, M. J. *J. Chem. Soc., Perkin Trans.* **1983**, 1863.
(35) Botulinski, A.; Buchler, J. W.; Tonn, B.; Wicholas, M. *Inorg. Chem.* **1985**, *24*, 3239.
(36) Abraham, R. J.; Marsden, I.; Xiujing, L. *Magn. Reson. Chem.* **1990**, *28*, 1051.
(37) Medforth, C. J.; Hobbs, J. D.; Rodriguez, M. R.; Abraham, R. J.; Smith, K. M.; Shelnutt, J. A. Submitted for publication.
(38) Barkigia, K. M.; Renner, M. W.; Furenlid, L. R.; Medforth, C. J.; Smith, K. M.; Fajer, J. *J. Am. Chem. Soc.* **1993**, *115*, 3627.
(39) Senge, M. O. *J. Chem. Soc., Dalton Trans.* **1993**, in press. Note that H_2OETNP, NiOETNP, and TlOETNP crystallize with two independent molecules in the unit cell which have different numbers of axial and equatorial ethyl groups.

interactions. Recently, substantial progress has been made in the development of a force field capable of accurately predicting the nonplanar structural distortions observed in the X-ray crystal structures of dodeca-substituted porphyrins.[12,16] These results were obtained using experimentally determined parameters in the force field (force constants from the NiOEP normal coordinate analysis and bond lengths and angles from the NiOEP triclinic B crystal structure),[20,27] rather than arbitrary adjustments of bond lengths and angles, to achieve an accurate representation of the nonplanar distortions. In this work, we have extended this approach by adding partial atomic charges and what is believed to be a more accurate van der Waals potential function to these calculations.[40] These modifications to the force field lead to more accurate predictions of the energies of various conformers, thus allowing the conformer with the lowest energy to be predicted. However, either form of this force field resulted in accurate predictions for the overall degree of nonplanar distortion resulting from steric repulsions between peripheral substituents on the nickel porphyrin.

In contrast to molecular mechanics calculations for NiOETPP,[12] calculations for NiOETNP suggest the presence of multiple isoenergetic conformers either having different ethyl-group orientations or displaying similar ethyl-group orientations but with differing modes of macrocyclic distortion (i.e. saddle or ruffled). In Figure 3, six of these conformers are shown. The top four structures possess different ethyl-group orientations, while the bottom two structures have the same ethyl-group orientation but display nearly identical energy minima with both saddle and ruffled conformations. These calculations suggest that, while the presence of four nitro groups causes significant distortion of the macrocycle, there is greater flexibility in the porphyrin core as compared to that of NiOETPP. This increased flexibility of the structure appears to affect the type of distortion (saddle or ruffled) rather than the degree of distortion (RMS OOP) observed. This result begs the question of how these two effects may be detected spectroscopically (see below). For instance, is resonance Raman spectroscopy sensitive to both the type and the degree of distortion in metalloporphyrins?

UV–Visible Absorption Spectra. Several studies have addressed the steric and electronic effects of *meso*-substitution upon the absorption, fluorescence, and redox properties in free base, diacid, and Zn *meso*-nitroporphyrin complexes in solution.[18,41] In particular, Gong and Dolphin[18i] noted a red shift and broadening of the major absorption bands, in both the metallated (Zn) and dication species, with increased *meso*-nitro substitution. They reasoned that the observed shifts were due to steric rather than electronic influences because absorption band shifts and broadening were more pronounced in the dication, which can distort more easily than the Zn OETNP. They also noted a similar effect in the absorption spectra for octamethyltetraphenylporphyrin and octaethyltetraphenylporphyrin resulting from steric crowding about the periphery of the porphyrin. Structurally induced red shifts in the UV–visible absorption spectra are further supported by INDO/CI molecular orbital calculations which demonstrate that increases in nonplanar distortions in the porphyrin macrocycle decrease the energies of the B and Q singlet states.[16] In contrast, it has been suggested that in porphyrins with *meso*-substituents of increasing electron-withdrawing ability the absorption bands are observed to shift to the blue.[42] Interpreted based upon the four-orbital model of Gouterman,[43] the blue shifts result from a lowering of the energy of the a_{2u} molecular orbital (HOMO), which has its greatest density at the methine carbons.

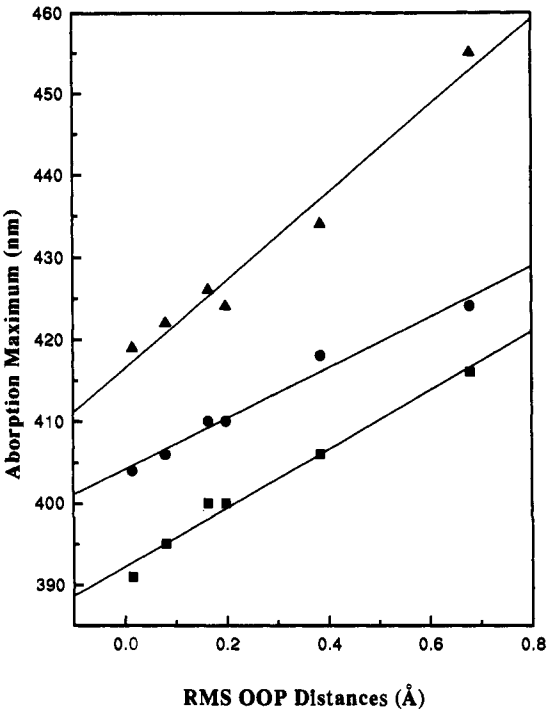

Figure 8. Positions of Soret absorption maxima for nickel(II) *meso*-nitroporphyrin derivatives in various coordinating and noncoordinating solvents plotted as a function of root-mean-square out-of-plane distances from the mean plane of the C_β, C_α, C_m, and N atoms of the porphyrin: ■, dichloromethane; ●, carbon disulfide; ▲, piperidine.

In the light of these two opposite effects, the observed red shifts in the UV–visible absorption spectra of the nickel(II) nitroporphyrin series must be caused by the sterically induced nonplanar distortions that are superimposed upon any competing blue shifts due to the strong electron-withdrawing capacities of the NO_2 substituents. The predominant influence of the nonplanar distortions on the absorption spectra for these derivatives is shown in Figure 8. Clearly, there is a strong linear dependence between total out-of-plane distances and wavelengths of the Soret absorption for the four-coordinate species. This correlation in somewhat less ($R = 0.98$) in the six-coordinate form. We suggest that the differences in the slopes and linear correlations observed in the six- versus four-coordinate forms of NiOETNP are due to changes in macrocyclic planarity induced by ligand binding. This effect is not evenly distributed between the *meso*-nitro derivatives. For example, binding of axial ligands to NiOEMNP changes the spin state and thus increases the core size of the nickel ion. The core expansion forces the macrocycle to adopt a more planar geometry and a less red-shifted absorption spectrum.[16] However, expansion of the porphyrin core will have less of an effect on porphyrin nonplanarity for NiOETNP, as compared to NiOEMNP, due to the greater steric constraints at the porphyrin periphery and thus results in less of a shift in the Soret absorption maximum.

The absorption bands in Figures 4 and 5 broaden significantly with increasing NO_2 substitution, especially evident for the Soret band. Also, for both the four- and six-coordinate forms, weak absorption bands to the blue of the Soret gain intensity with increased NO_2 substitution. These bands are particularly apparent in the spectra of the six-coordinate species where the spectrum of the NiOETNP(pip)$_2$ complex becomes hyper in character.[19,44] INDO/s calculations indicate that porphyrin-to-nitro charge-transfer transitions gain significant oscillator strength in this region of the electronic spectrum of NiOETNP.[25] The broadening of the absorption bands may result from band splitting or inhomogeneity induced by the NO_2 substituents.

(40) Mayo, S. L.; Olafson, B. D.; Goddard, W. A., III. *J. Phys. Chem.* **1990**, *94*, 8897.
(41) Wu, G.-Z.; Gan, W.-X.; Leung, H.-K. *J. Chem. Soc., Faraday Trans.* **1991**, *87*, 2933–2937.
(42) Meot-Ner, M.; Adler, A. D. *J. Am. Chem. Soc.* **1975**, *97*, 5107–5111.
(43) Gouterman, M. In *The Porphyrins*, Dolphin, D., Ed.; Academic Press: New York, 1978; Vol. 3, Chapter 1.
(44) Gouterman, M.; Hanson, L. K.; Kahlil, G.-E.; Leenstra, W. R.; Buchler, J. W. *J. Chem. Phys.* **1975**, *62*, 2343.

Although band splitting, due to the removal of the degeneracy of the x and y components of the transition dipole of the porphyrin by addition of one, two, or three nitro groups, is possible, this explanation is unlikely because this band broadening is greater for NiOETNP, which has equivalent x and y dipoles. Thus, an increase in structural inhomogeneity is the probable origin of this effect (see below).

NMR Spectra. Several recent NMR studies have probed the conformations of nonplanar dodeca-substituted porphyrins in solution using variable-temperature NMR spectroscopy.[30] These studies have shown that in many cases the porphyrin macrocycle inverts between nonplanar conformations. Not surprisingly, the barrier to inversion is highly dependent upon the steric interactions among peripheral substituents and, for the free base and dication, among the hydrogens attached to the pyrrole nitrogen atoms. One dodeca-substituted porphyrin which is closely related to OETNP and which has been extensively studied is 2,3,7,8,12,-13,17,18-octaethyl-5,10,15,20-tetraphenylporphyrin (OETPP). It was of interest to compare the solution conformations of the OETNP complexes, as determined by variable-temperature NMR spectroscopy, with the results previously obtained for OETPP complexes.[30b]

H_2OETPP displays two dynamic processes $\Delta G^*_{293} = 13.7$ kcal mol^{-1} and $\Delta G^*_{383} = 18.1$ kcal mol^{-1}. The process with the lower energy barrier was determined to be NH tautomerism.[30b] Therefore, changing the *meso*-phenyl rings to nitro groups does not significantly alter the value of ΔG^* for NH tautomerism. The second dynamic process observed for H_2OETPP caused the methylene protons to become diastereotopic and was assigned as macrocyclic inversion.[30b] A similar process was seen for NiOETPP ($\Delta G^*_{293} = 13.2$ kcal mol^{-1}), ZnOETPP(pyridine) ($\Delta G^*_{345} = 16.2$ kcal mol^{-1}), and H_4OETPP^{2+} ($\Delta G^* > 20$ kcal mol^{-1}). In contrast, macrocyclic inversion was not observed for H_2OETNP, H_4OETNP^{2+}, and NiOETNP. This suggests that the barrier to any fluxional process in the OETNP complexes is significantly lower (probably by at least 10 kcal mol^{-1} for the free bases and dications) than in the OETPP complexes. The lower ΔG^* values of the OETNP complexes may be interpreted in terms of a reduction in the steric repulsions between the peripheral substituents, especially the interactions of the methyl hydrogens with the *meso*-substituents. This reduction in peripheral steric strain leads to an increase in the conformational freedom of the OETNP macrocycle versus the OETPP macrocycle.

Raman Spectra. Increased nonplanarity of the porphyrin core upon *meso*-substitution is supported by the resonance Raman spectra (Figure 6 and Table 3). As compared to the parent compound, NiOEP, all the structural marker modes (ν_{10}, ν_2, ν_3, and ν_4) shift to lower frequencies with *meso*-substitution. A similar pattern was noted for a series of octaalkyltetraphenylporphyrins where increasing steric interactions among the peripheral substituents lead to increased macrocyclic distortion.[12] A curious exception to this general pattern of Raman shifts (in response to increasing porphyrin nonplanarity) is noted for NiOE5,15DNP, where ν_2 appears to be split into two modes of unequal intensities. Further inspection reveals the presence of similar, although weaker, coupling of modes in the ν_2 region for mono- and trinitro-substituted NiOEP. Other Raman modes appear to be affected as well; in particular, the position of the putative asymmetric NO_2 at 1540 cm^{-1} in NiOEMNP is sensitive to this coupling (i.e. this mode appears at lower frequencies for cases in which apparent splittings occur). At this time, the origin of this coupling is not readily apparent. It is also interesting to note that ν_{10}, which is a strong depolarized mode in NiOETNP, is absent in the Raman spectrum of the tetraphenyl-substituted OEP.

The presence of an additional Raman active mode at approximately 1360 cm^{-1} in the spectra of each of the nitro-substituted porphyrins has been tentatively assigned as the symmetric NO_2 stretch.[11] The position of this mode is also influenced by the porphyrin conformation (see Figure 6 and Table 3) and shifts to lower frequency with increasing substitution. This shift may be precipitated by ruffling and/or saddle distortion of the macrocycle, which may in turn increase interactions between the π orbitals of the porphyrin and the π^* orbitals of the NO_2 group. Such interactions could lead to electron donation from the porphyrin π orbitals to the π^* orbitals of NO_2, thus increasing the antibonding character of these orbitals and resulting in decreased vibrational frequencies.

Structural Heterogeneity. Evidence for heterogeneity in the degree of nonplanarity for some members of the *meso*-nitro-substituted series is present in the resonance Raman spectra. As was previously observed in the Raman spectra of NiOEP, ν_{10} is the most affected by the existence of structural conformers differing in planarity because of the large shifts in this line resulting from nonplanar distortion.[11,28] ν_{10}, for NiOEP, can be decomposed into two component modes that are assigned to (high frequency) planar and (low frequency) nonplanar forms. A similar analysis can be applied to the spectra for the mono-, di-, and trinitro-substituted species (decompositions shown in Table 3) which clearly shows broad asymmetric line shapes for ν_{10}.

Raman data indicate heterogeneity in the degree of distortion for all but NiOETNP. Curve fitting suggests that, while NiOEP exists in solution as approximately equal mixtures of planar and nonplanar forms, substitution of one or more nitro groups causes the nonplanar forms to dominate. This analysis also indicates that, for NiOETNP, a high-frequency, less ruffled form cannot be rationalized. However, the observed variety of ethyl orientations in the crystal structures of OETNP complexes[39] suggests that NiOETNP may also exhibit structural heterogeneity, if not in the *degree* of distortion, then in the *type* of distortion. Heterogeneity in the type of distortion is supported by the effect of ethyl orientation of the low-energy conformers predicted in the MM calculations. The variable-temperature NMR studies are also consistent with the conformational flexibility of the OETNP macrocycle suggested by the molecular mechanics calculations. Lastly, the progressive broadening of the absorption bands with successive nitrosubstitution may be a result of multiple conformers differing in the type of distortion, but not the degree of macrocyclic distortion.

Plots in Figure 9 of calculated RMS OOP versus Raman frequencies of the primary structural marker lines suggest a strong correlation between out-of-plane distortion of the macrocycle and the observed porphyrin vibrations. Similar plots of specific structural parameters such as calculated core size or twist angle versus Raman frequency demonstrate much weaker direct correlations. This finding indicates that the frequencies of Raman structural marker modes in the nitro OEP series are determined by total nonplanar distortion rather than the specific type of distortion. The results of absorption, Raman, variable-temperature NMR, and molecular mechanics calculations for the OETPP and OETNP complexes all suggest the possibility of structural heterogeneity. Further, published crystallographic data for NiOETPP,[38] CoOETPP,[16] CuOETPP,[16] and ZnOETPP[30b] and preliminary X-ray structures[39] of H_2OETNP, ZnOETNP, NiOETNP, and TlOETNP all show highly nonplanar saddle conformations. However, the structures of the OETPP and OETNP complexes differ in that the OETNP complexes show heterogeneity in the orientations of the ethyl groups.[39] Moreover, in contrast to NiOETPP, the energy-optimization calculations give a wide range of nonplanar structures with similar energies.

Axial Coordination. The strong electron-withdrawing character of the nitro groups has a marked effect on the coordination chemistry, progressively enhancing the relative affinity of the nickel ion for axial ligands. For example, in piperidine, both four- and six-coordinate forms are observed in the absorption spectrum of NiOEP whereas for NiOEMNP only the six-coordinate species is present. The further enhancement of ligand

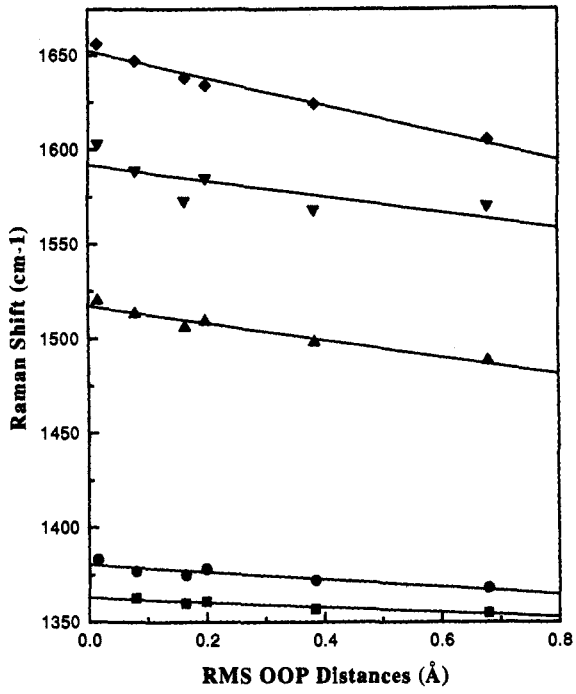

Figure 9. Positions of maxima of various Raman lines for nickel(II) *meso*-nitroporphyrin derivatives plotted as a function of root-mean-square out-of-plane distances from the mean plane of the C_β, C_α, C_m, and N atoms of the porphyrins: ■, ν_{NO_2}; ●, ν_4; ▲, ν_3; ▼, ν_2; ◆, ν_{10}.

affinity by additional nitro substituents is most evident for NiOETNP, which is found to bind weak σ-donating ligands such as methanol. These results argue that a significant electronic effect from the nitro substituent is transmitted to the central metal, increasing its positive charge. This finding has significant bearing on axial ligand binding in nonplanar nickel porphyrins and chlorins such as those present in methylreductase cofactor F_{430}.[14]

The binding of axial ligands results in a change in spin state of the nickel ion. (The unligated form has a $S = 0$ spin state, while the ligated species has $S = 1$). This spin-state change is reflected by the red shift in the absorption bands upon ligand binding relative to the unligated form (Table 2). As in the spectra of the four-coordinate species, the absorption spectra of the six-coordinate species are further red shifted with increased *meso*-nitro substitution. This is demonstrated in Figure 8 by the plots of Soret band positions versus RMS OOP distances for the *meso*-nitro-substituted OEP series. The slopes of the resulting lines for the two noncoordinating solvents are similar and suggest that increased steric interactions due to *meso*-substitution result in similar structural changes to the macrocycle. In contrast, in a coordinating solvent such as piperidine, larger structural changes result, for a given degree of *meso*-substitution, because of the increased size of the high-spin nickel ion. This increase in effective metal size probably results in a more planar macrocycle, especially for the nonplanar conformers of four-coordinate OEP and for mono- and dinitroporphyrins. The more highly substituted tri- and tetranitro OEPs are not as likely to assume planar conformations upon ligand binding. Therefore the magnitude of the overall shift induced by ligand binding results from two contributions: (1) a red shift due to ligand addition and (2) a blue shift due to the increase in planarity of the conformers. The difference in contributions by these sources causes the apparent larger slope of the line for the six-coordinate complexes.

Conclusions

The *meso*-nitrooctaethylporphyrins provide an interesting series of compounds in which steric and electronic effects produced by nonplanar distortions and the presence of strong electron-withdrawing groups may be systematically investigated. This study shows that increasing steric repulsion at the porphyrin periphery increases nonplanar distortion, a trend which is predicted by molecular mechanics calculations. Raman marker lines were also found to accurately predict the degree of distortion present in this series. The Raman spectra suggest heterogeneity in the type of structural distortion found for the mono-, di-, and trinitro-substituted octaethylporphyrins. Structural heterogeneity is not observed in the Raman spectra of NiOETNP, although both MM calculations and Raman evidence successfully measure the degree of nonplanar distortion for this compound. However, NMR results and MM calculations support multiple macrocyclic conformers for NiOETNP. UV–Visible absorption spectra of the bis-ligated forms of this series display a hyper character in the Soret region of the spectra. INDO/CI calculations indicate that these bands arise from porphyrin-to-nitro group charge-transfer transitions. Axial ligand affinity is influenced by both electronic and conformational effects; for this series, these effects cannot be completely separated. Therefore, we are currently examining axial ligand affinity for a series of dodecaphenylporphyrins where the degree of macrocycle distortions among increasingly halogenated species is fairly constant.

Acknowledgment. Work performed at Sandia National Laboratories was supported by U.S. Department of Energy Contract DE-AC04-94AL85000 and the Associated Western Universities, Inc. (postgraduate fellowships to J.D.H., S.A.M., and C.J.M.). We thank Dr. Mathias Senge for a preprint of ref 39.